Pediatric Radiology (2020) 50:1293–1307
https://doi.org/10.1007/s00247-020-04684-3

PICTORIAL ESSAY

Computed tomography and magnetic resonance imaging in pediatric salivary gland diseases: a guide to the differential diagnosis

Felice D'Arco[1] · Lorenzo Ugga[2]

Received: 9 March 2020 / Revised: 9 March 2020 / Accepted: 16 April 2020 / Published online: 18 June 2020

Abstract
Salivary gland pathologies in children are frequent, particularly viral infections, but rarely need cross-sectional imaging. However, when a mass involves the salivary spaces (primarily or as a secondary invasion from other neck spaces) it may pose problems in the differential diagnosis and in immediate management. Infrequently, systemic autoimmune diseases can also involve the salivary parenchyma in children and correctly interpreting the constellation of findings in the whole body is critical for the diagnosis. Distinguishing between cystic and solid masses is the first step for radiologists in order to narrow down the diagnosis. Location and spatial extension are the most important elements differentiating cystic masses, while signal characteristics, internal structure and local invasion help in the differential diagnosis of solid masses.

Keywords Benign tumor · Child · Computed tomography · Congenital malformation · Differential diagnosis · Infection · Inflammation · Magnetic resonance imaging · Neoplasia · Salivary glands

Introduction

The most common salivary gland pathologies in children are viral infections, but apart from those, salivary gland diseases in children are rare and may pose a problem in terms of differential diagnosis. In this review, we describe: 1) the relevant anatomy of the parotid, submandibular and sublingual spaces; 2) inflammatory diseases, 3) congenital conditions and 4) masses involving the salivary spaces/glands with a focus on the elements of radiologic differential diagnosis.

Congenital anomalies can be associated with a specific syndromic constellation of findings and/or genetic causes that should be taken into account by radiologists. Inflammations and infections are often nonspecific on imaging while masses involving salivary gland spaces follow imaging features of the same entities involving other neck spaces. Distinguishing between cystic and solid masses is the first step for radiologists in order to narrow down the diagnosis. Location and spatial extension are the most important elements differentiating cystic masses, while signal characteristics, internal structure and local invasion help in the differential diagnosis of solid masses.

This paper is intended as a simple guide for general radiologists and trainees toward the correct interpretation of pediatric salivary gland disease.

Anatomy

The salivary glands comprise the paired parotid, submandibular and sublingual glands, referred to as the major salivary glands, together with submucosal clusters of salivary tissue scattered around the oral cavity, paranasal sinuses, pharynx and upper respiratory tract (minor glands).

Parotid space

The superficial layer of deep cervical fascia delimits the parotid space in the lateral suprahyoid neck. This space is related to the parapharyngeal space medially, the masticator space anteriorly

✉ Felice D'Arco
felice.darco@gosh.nhs.uk

[1] Department of Radiology, Neuroradiology Unit, Great Ormond Street Hospital for Children NHS Foundation Trust, Great Ormond Street, London WC1N 3JH, UK

[2] Department of Advanced Biomedical Sciences, University of Naples "Federico II", Naples, Italy

and the carotid space posteromedially. Inferiorly, the parotid tail extends into the posterior submandibular space (Fig. 1).

The parotid space is divided into superficial and deep compartments by the facial nerve or by a line between the stylomastoid foramen and the lateral margin of the retromandibular vein.

The superficial parotid gland lies below and anterior to the external auditory canal, superficial to the masseter muscle. The deep portion of the gland extends medially through the stylomandibular tunnel between the mandibular ramus and the anterior edges of the sternocleidomastoid muscle and the posterior belly of the digastric muscle. In about one-fifth of subjects, an accessory lobe, lying superficial to the masseter muscle, can be appreciated.

In addition to the parotid gland, the parotid space contains other critical anatomical structures, including the facial nerve, the external carotid artery, the retromandibular vein and intraparotid lymph nodes.

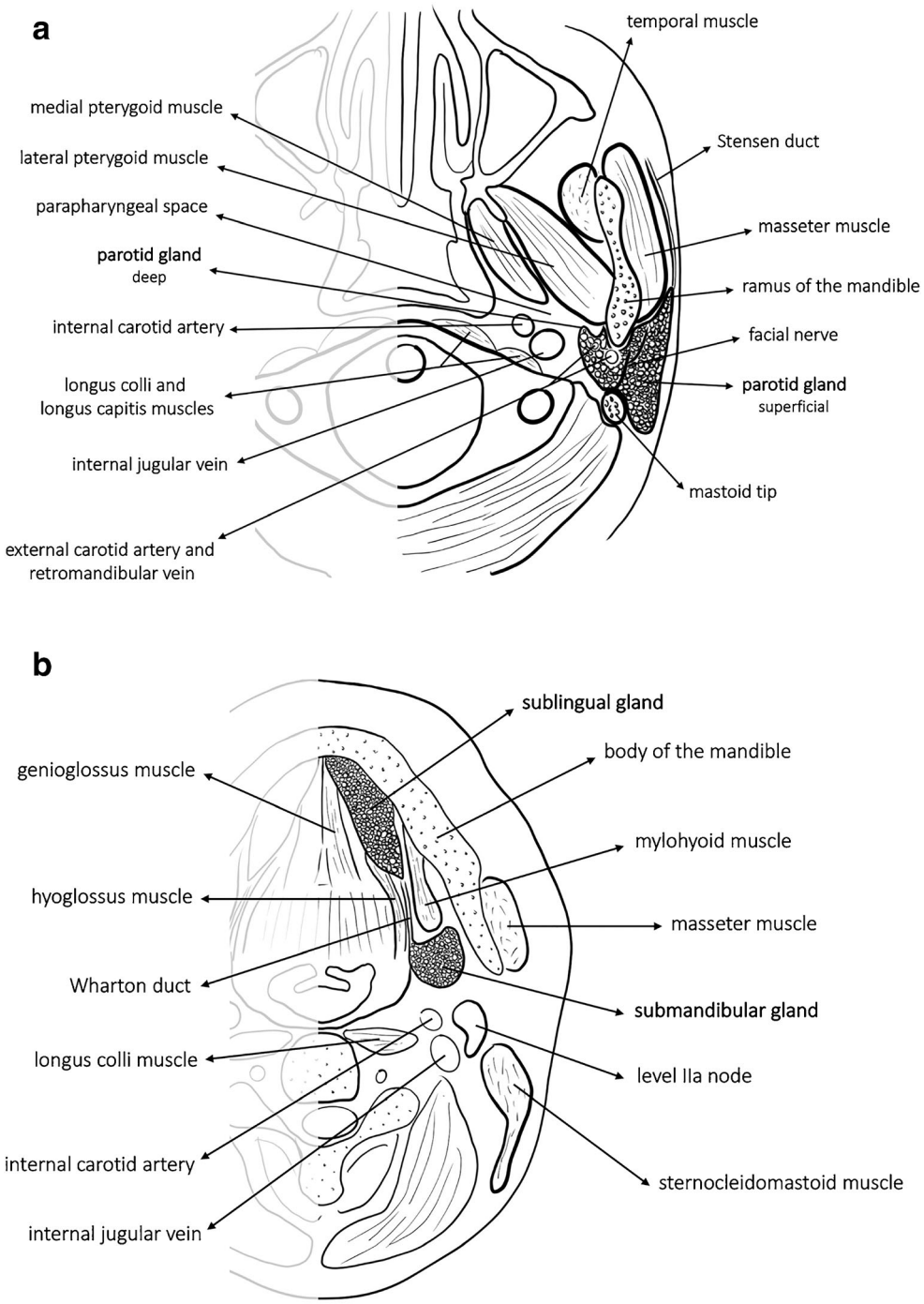

Fig. 1 Anatomy of the salivary glands. **a** Axial drawing depicts the parotid space and its relationship with surrounding neck spaces. **b** Axial drawing depicts submandibular and sublingual glands and their anatomical relationship

The parotid duct (Stensen duct), which arises from the anterior aspect of the gland, runs over the masseter and pierces the buccinator to open in the buccal vestibule at the level of the second upper molar.

The facial nerve emerges from the stylomastoid foramen of the skull, courses laterally around the styloid process superficial to the posterior belly of the digastric muscle. It continues caudally within the parotid gland, dividing into an upper trunk, giving off its temporal and zygomatic branches, and lower division, which breaks up into its buccal, mandibular and cervical branches.

The auriculotemporal nerve, branch of the mandibular nerve, represents another nervous structure included in the parotid space, which penetrates the gland posteriorly to the mandibular condyle carrying secretory fibers.

Submandibular space

The submandibular space is a superficial space above the hyoid bone inferolateral to the mylohyoid muscle containing the submandibular gland, facial vessels, nodes and the anterior belly of digastric muscle.

The submandibular gland, the second largest salivary gland, is folded around the dorsal free edge of the mylohyoid muscle from which it is divided into a superficial and a deep portion. The superficial portion, covered by the superficial layer of the deep cervical fascia, lies in the submandibular space bounded by the digastric, the stylohyoid and the medial pterygoid muscles. Superiorly, the stylomandibular ligament separates it from the parotid gland whereas the mylohyoid and hyoglossus muscles border the floor of the submandibular space deeply (Fig. 1).

The anterior facial vein runs superficial and lateral to the submandibular gland, where it has been suggested as a landmark to help differentiate intra- and extra-glandular lesions. Indeed, primary diseases of the gland are never separated from the gland by the vein whereas the vein separates lymphadenopathy from the glandular parenchyma [1, 2]

Beyond the posterior edge of the mylohyoid muscle, the deep portion of the submandibular gland extends in the floor of the mouth (i.e. sublingual space). At this level, the lingual nerve runs lateral to the gland, while the hypoglossal nerve lies medially. Wharton duct exits the gland anteriorly, extends between the sublingual gland and the genioglossus muscle and terminates in the anterior floor of the mouth.

Sublingual space

The sublingual space is a non-fascial lined space lying superomedial to the mylohyoid muscle. It communicates with the contralateral sublingual space on the midline and with submandibular space posteriorly through the edge of the mylohyoid muscle. This space contains the sublingual gland and ducts, the deep portion of the submandibular gland, and Wharton duct, hypoglossal and lingual nerve laterally and glossopharyngeal nerve and lingual vessels medially (Fig. 1).

A possible communication between submandibular and sublingual spaces is represented by congenital defects of the mylohyoid muscle. They present a relatively high incidence (35–50%) and may contain the sublingual gland or sometimes blood vessels and fat [3].

Diagnostic work-up

Clinical history and physical examination are essential in evaluating patients with salivary gland disorders as they are crucial to address the diagnostic work-up and formulate the differential diagnosis. The acute onset or long persistence of gland swelling, the rate of change in the gland size and associated symptoms should be carefully assessed. Physical examination includes inspection of the face and oral cavity, and massage of the gland to measure tenderness and determine the size and texture of the gland.

In the setting of acute swelling of parotid glands, a viral infection is the most probable etiology and imaging is usually not indicated. On the contrary, in case of acute swelling of a single major salivary gland, particularly when associated with fever and pain, an acute suppurative sialadenitis should be suspected. Ultrasound (US) represents the first-level imaging modality, while contrast-enhanced computed tomography (CT) should be carried out in the suspicion of complications, such as abscess or jugular thrombosis. A chronic generalised swelling of major salivary glands can indicate different causes. Its association with systemic symptoms or adenopathies may raise the suspicion of chronic sialadenitis, including HIV-related and mycobacterial sialadenitis. Also for this condition, US is indicated while magnetic resonance imaging (MRI) may help obtain a panoramic view and better characterisation. For the same reasons, US and then MRI should be performed in case of chronic swelling of a single major salivary gland, which may be caused by cystic lesions, vascular abnormalities or neoplasms [4].

Congenital and genetic abnormalities of the salivary glands

Salivary gland aplasia

Salivary gland aplasia (or agenesis) is a rare condition of unclear etiology in which one or multiple major salivary glands are congenitally absent. It affects the parotid or submandibular glands and may be unilateral or bilateral.

Salivary glands form through the growth of buds from the oral epithelium into underlying mesenchyme during embryogenesis. The parotid secretory tissue is of

ectodermal origin while the submandibular, sublingual and minor salivary glands have endodermal origin.

Parotid gland primordia (anlagen) arise in weeks 5–6 of gestation, followed by submandibular and sublingual ones in weeks 6 and 7–8, respectively; minor salivary glands develop during the third month [5].

Although the parotid primordia are the first to appear, their encapsulation by the superficial layer of the deep cervical fascia of the neck develops after that of the submandibular and sublingual glands and after development of the lymphatic system (between the 12th and 14th fetal weeks). This results in intraparotid lymph nodes, which are normally absent in the other major salivary glands [6].

The absence of both parotid glands has been observed in lacrimo-auriculo-dento-digital syndrome (autosomal dominant) [7], in hypoplasia of the lacrimal glands or absence of lacrimal puncta [8], in hemifacial microstomia and in ectodermal dysplasia. Salivary gland aplasia has also been reported in Down syndrome [9], Klinefelter syndrome [10] and SOX10 mutation, which is characterised by inner ear dysplasia, absent olfactory bulbs (Kallmann disease), absent lacrimal glands and absent ganglionic cells in the bowel (Hirschsprung disease) [11] (Fig. 2). Furthermore, it may be associated with first branchial arch defects in Treacher Collins syndrome (mandibulofacial dysostosis) [12].

Unilateral forms may be associated with compensatory hypertrophy of the other salivary glands, in particular sublingual glands, and are usually asymptomatic. In these cases, the suspicion should arise for asymmetrical parotid or submandibular areas. The absence of Stensen duct papilla on clinical examination could be helpful for unilateral parotid aplasia diagnosis [13]. In bilateral forms, the severe lack of saliva leads to dental caries, periodontal disease and candidiasis [14].

On imaging, the absence of a parotid or submandibular gland should be differentiated from an atrophic gland secondary to obstruction of the secretory system, in which end-stage fat completely replaces the gland.

Lastly, one or both of the submandibular glands can sometimes be situated lower than normal configuring a developmental variant without pathological significance.

Salivary gland hypoplasia

Hypoplasia of the salivary gland can be sporadic or genetic (autosomal dominant) and may be associated with lacrimal gland hypoplasia. In sporadic cases, the association with Goldenhar syndrome is important: unilateral abnormal development of the nose, soft palate, ear and otic capsule, mandible and lips. Genetic cases have been associated with mutation in FGF10 gene [15].

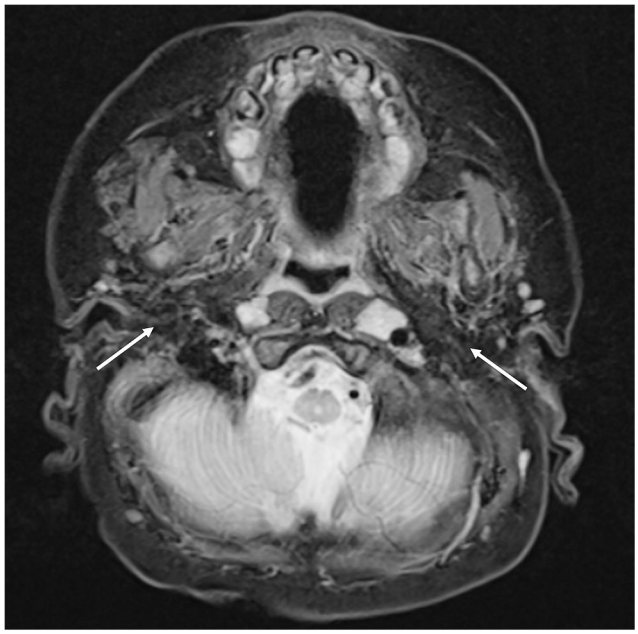

Fig. 2 Axial T2-weighted image with fat suppression shows bilateral absence of the parotid glands (*arrows*) in a 34-week-old girl with SOX10 mutation

Polycystic dysgenetic disease of the parotid gland

This is an extremely rare genetic disorder (possibly autosomal dominant) presenting in women during childhood or early adulthood. This condition is likely due to a developmental defect in the ductal anatomy with replacement of the lobular areas of the parenchyma by several epithelial cysts originating from the ducts. The cysts may contain microliths and the natural evolution of the disease is toward fibrosis and atrophy. Clinically, there is intermittent and painless swelling of the glands and MRI in a few reported cases with images showed well-circumscribed glands with diffuse enlargement, abnormal inhomogeneous signal and multiple very small internal cysts [16]. Reports of images are scarce, diagnosis is histological and image findings nonspecific.

Cystic lesions

First branchial cleft cyst

The branchial arches are the embryological precursors from which many of the adult structures of the head and neck arise. In detail, six pairs of branchial arches develop from the pharyngeal foregut between the 4^{th} and 7^{th} weeks of gestation. Each arch is externally lined by an ectoderm recess (branchial cleft) and internally by a layer of endoderm (branchial pouch) between which is a core of mesenchyme [17].

Each arch is associated with a central supporting cartilaginous portion, an aortic arch artery and a cranial nerve, which is the trigeminal nerve for the 1st arch [18].

The first pharyngeal cleft forms the external auditory meatus, while the corresponding pouch gives rise to the middle ear and eustachian tube. The tympanic membrane derives from the confluence of these structures and therefore comprises ectoderm, mesoderm and endoderm. Distally, the first branchial arch forms the mandibular and maxillary processes, and the muscles of mastication, malleus and incus [19].

First branchial cleft anomalies include cysts, sinuses or fistulae in the region of the angle of the mandible, accounting for fewer than 8% of all branchial abnormalities. They are classified as Type I or Type II based on presumed pathogenesis but with limited imaging applicability. Type I is considered ectodermal in origin and presents as cystic masses adjacent to the external auditory canal. In particular, it is located in the postauricular area, medial, inferior and posterior to the pinna and concha extending superiorly in proximity to the main trunk of the facial nerve. On the other hand, Type II anomalies, both ectodermal and mesodermal in origin, include cysts, sinuses or fistulae between the external auditory canal and submandibular area [18].

They present with cervical swelling and drainage from a skin depression at the angle of the mandible or the external auditory canal, which may be purulent if infected.

CT and MRI demonstrate an unilocular or multilocular cystic mass adjacent to the parotid gland, which is occasionally associated with a tract terminating along the external ear canal or middle ear (Fig. 3). Cyst wall thickening and enhancement may be depicted in cases of infection. Fat-suppressed post-contrast MR images are useful to demonstrate the tract. Differential diagnoses include parotitis with abscess formation, lymphatic malformation, sialocele and benign lymphoepithelial cyst [20, 21].

Surgical excision represents the definitive treatment for first branchial cleft anomalies, typically complicated by recurrent infections. A sinogram may be preoperatively performed to delineate the extent of the tract.

Lymphatic malformation

See noninflammatory masses of the salivary glands.

Ranula

Ranulas are mucoceles that form following obstruction of or trauma to the sublingual gland. For this reason, they represent pseudocysts rather than real cysts, which are characterized by an epithelial wall. The most common type is the simple ranula (or oral ranula), which develops above the mylohyoid muscle in the floor of the mouth and clinically presents as an intraoral swelling. The less frequent plunging ranula (or diving ranula) extends through a defect of the mylohyoid muscle in the submandibular space, causing a submandibular and/or submental bump with or without intraoral swelling. Submandibular extension may also occur through the physiological communication between the submandibular and sublingual spaces at the posterior edge of the mylohyoid muscle (Fig. 4).

US is useful to confirm the cystic nature of the lesion and to identify mylohyoid defects. On CT, ranulas appear as well-defined unilocular cystic lesions with low attenuation, while MR features are low signal on T1-weighted and high signal on T2-weighted images, which can variate depending on the protein concentration. Infected ranulas may show peripheral enhancement. In plunging ranulas, the sublingual space's collapsed component is commonly referred to as the tail sign.

Ranula differential diagnoses include cystic lesions of the floor of the mouth such as epidermoid/dermoid cysts and lymphatic malformations [22, 23].

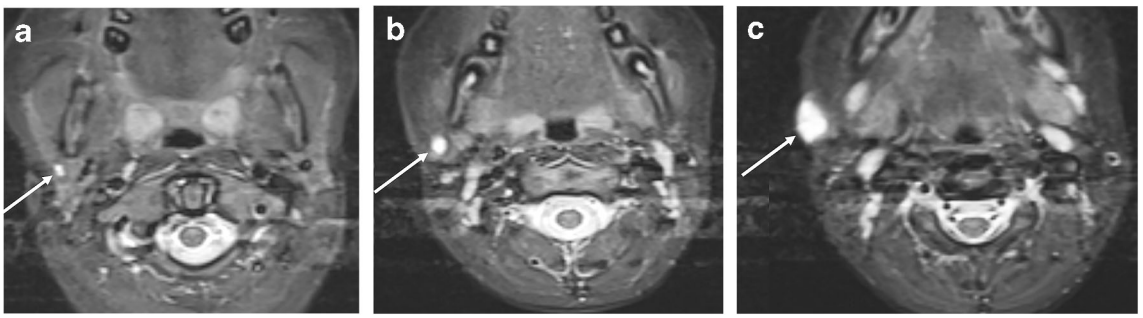

Fig. 3 Axial STIR (short tau inversion recovery) images of a first branchial cleft anomaly Type II in a 10-year-old girl. **a–c** Serial section in the craniocaudal direction shows a tract (*arrows*) from within the right parotid gland (**a**), passing the angle of the mandible (**b**), and terminating in a cyst within the subcutaneous fat of the right submandibular region (**c**)

Fig. 4 Axial T1-weighted image in a 14-year-old boy shows a left plunging ranula extending in the submandibular space. The ranula shows increased T1 signal consistent with highly proteinaceous fluid. Note the normal submandibular gland on the right (*arrow*)

Acquired immunodeficiency syndrome-related parotid cysts

Acquired immunodeficiency syndrome (AIDS)-related cysts usually present as bilateral parotid cystic lesions, even in the presence of a unilateral clinical involvement. Cervical lymphadenopathy due to human immunodeficiency virus (HIV) infection as well as solid benign lymphoepithelial lesions are often observed in these patients. AIDS-related cysts are histologically lined by squamous epithelium associated with reactive lymphoid stroma.

US and cytological examination are sufficient to confirm the diagnosis in HIV-positive patients. CT and MRI may be useful to depict deep parotid cysts, possibly extending into the parapharyngeal space and compressing oropharynx [24]. A thin rim enhancement is usually depicted.

Solid accompanying lymphoepithelial lesions show diffusion restriction with variable heterogeneous enhancement [25, 26].

Inflammation and infection

Imaging findings in inflammations and infections of the salivary glands in children are nonspecific and often not necessary. Clinical context is paramount for the correct diagnosis and management.

Acute infections of the salivary glands

The most common salivary viral infection in the pediatric population is caused by mumps and is characterized by bilateral enlargement of the salivary gland (particularly the parotid glands) while *Staphylococcus aureus* is the most common cause of acute bacterial infection [27]. Imaging is not necessary and the diagnosis is clinical [28].

CT and MRI show diffuse enlargement of the glands with some increased hypodensity (on CT) or increased T2-weighted images signal (on MRI) due to oedema [29]. Internal fluid collection can be seen in both MRI and CT as well as dilatation of the Stensen duct. Enlarged lymph nodes can be present. It is important to note that pyogenic infections can be responsible for abscesses in the salivary glands that can be seen as fluid collections surrounded by rim enhancement on CT and presenting with restricted diffusivity of the fluid core (pus) on MRI [30]. Acute infection of the parotids is characterised clinically by fever and painful swelling.

The main differential diagnoses in bilateral swelling of the parotid glands are: 1) HIV-related sialopathy, 2) chronic infections and 3) autoimmune disease such as juvenile Sjögren disease, IgG4 related disease and others.

Chronic sialadenitis in childhood

Sialadenitis is considered chronic when acute episodes recur with clinical manifestation of swelling, pain and fever interspersed with asymptomatic periods. Chronic juvenile recurrent parotitis is more common than adult chronic parotitis and involves children between 3 and 6 years of age and over time the swelling persists while the pain reduces [31]. CT and MRI are nonspecific, showing enlargement of the salivary glands and heterogeneous density/intensity evolving in an atrophic picture [32, 33]. Internal calcifications, nodal enlargement, dilatation of the Stensen duct and multiple foci of hyperintensity in T2-weighted imaging can be seen [27, 31] (Fig. 5).

Tuberculosis and other mycobacteria

Mycobacterial involvement of the salivary gland is rare in children and is normally seen in adults between 20 and 30 years of age, with the parotid gland being the most common site of involvement (70%) followed by the submandibular and sublingual glands [31]. Atypical mycobacteriosis is radiologically similar to tuberculosis and both present with enlargement of the glands, reactive nodes, calcifications, abscesses/tuberculomas and necrotic areas. In most cases, the parotid involvement

Fig. 5 Chronic parotitis in an 8-year-old boy. Coronal T2 STIR (short tau inversion recovery) shows enlargement of the left parotid gland (*arrow*) with multiple small foci of T2 hyperintensity

represents the extension of the cervical nodes' infection [31, 34–36]. Tuberculomas can present as low T2-weighted image areas, which is quite typical of granulomatous processes in head, neck and brain imaging and allows, to some extent, differentiation from pyogenic abscesses [37]. Diffuse, nodular or rim enhancement can be seen [34]. On US, hypoechoic nodules with associated calcified areas are seen [36].

Juvenile Sjögren disease

Sjögren disease is an autoimmune and chronic inflammatory disorder of the salivary and lacrimal glands characterized by diffuse lymphocytic infiltration of the parenchyma. In these patients, bilateral parotid enlargement is often associated with abnormal dryness of the conjunctiva and cornea of the eye (xerophthalmia) and dry mouth (xerostomia) [38].

Juvenile Sjögren disease is poorly defined and most likely an underdiagnosed condition. The first presentation is often with bilateral swelling of the parotid glands and or presumed diagnosis of recurrent parotitis and the age at the diagnosis is around 10 years [39]. It is important, in patients with bilateral parotid swelling or sign/symptoms suggesting Sjögren disease, to look for systemic clinical manifestations that are common in those patients, including hematological, neurological, vascular, musculoskeletal and respiratory symptoms that are present in up to 50% of the patients [38].

On US, salivary glands appear either normal (particularly in the acute phase) or may demonstrate typical diffuse multicystic pattern [40].

Typically, CT also shows multicystic areas alternating with a solid glandular component (reticular pattern) with associated foci of calcifications. On MRI, the imaging characteristics are similar with the cystic appearance of the gland that changes with time, being microcystic at the beginning and evolving into larger cysts (Fig. 6). It is important to know that solid areas due to lymphocytes aggregation can simulate a tumor particularly in post-contrast sequences and in diffusion-weighted images. In the parotid glands when the cysts are larger than 2 mm, this is considered an advanced macrocystic stage of the disease. In a child with suspected Sjögren disease, an MRI sialography needs to be considered: the main radiologic findings are changes in the parotid ducts, which may be punctate in the early stages and progress toward more globular, cavitary and destructive abnormalities [41]. Lacrimal glands may also be

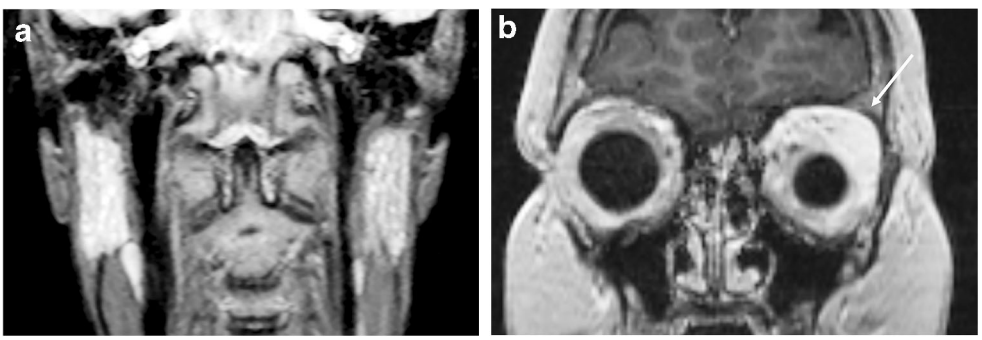

Fig. 6 Juvenile Sjögren disease in an 11-year-old girl presenting with intermittent swelling of the parotids. **a** Coronal T2 STIR (short tau inversion recovery) shows microcystic appearances of the parotid glands. **b** Coronal T1-weighted image post injection of gadolinium shows enlargement of the left lacrimal gland (*arrow*)

involved and can be hypertrophic or atrophic [42] (Fig. 6). Very rarely, Sjögren disease can present with ranula in the floor of the mouth [43] or can involve cranial nerves presenting as polyneuropathy.

Radiologically, other multicystic masses involving the parotid need to be considered in differential diagnosis, particularly a lymphatic malformation that can be micro- or macrocystic and is far more common in children. In these cases, clinical presentation is different with progressive swelling and without inflammatory symptoms. Furthermore, a lymphatic malformation does not have solid components, is transpatial extending beyond the parotid space and is unilateral without associated systemic involvement.

Immunoglobulin G4-related disease

Immunoglobulin G4 (IgG4)-related disease is an autoimmune disorder that involves several organ systems and is characterized by high levels of IgG4 in the blood and infiltration/fibrosis of several organs due to plasma cells expressing IgG4. It is considered an adult disease and literature on the pediatric population is scarce. However, children may be affected and some pediatric cases can present as a solid lesion simulating a tumor [44]. To consider this entity in the differential diagnosis of inflammatory processes involving salivary glands is important because if not treated it can lead to irreversible fibrotic damage. Prednisolone is the first-line therapy and shows resolution of the symptoms in most cases. Chronic sclerotising sialadenitis was historically called Kuttner tumor; it is now known that this is due to IgG4-related disease [45, 46].

Radiologically, US can demonstrate enlargement of salivary glands, as well as the presence of reactive enlarged lymph nodes (i.e. diffuse hypoechogenicity but preserved hilum and hilar vascularity). Interestingly, salivary gland involvement has been described as inhomogeneous with some part of the gland more involved than the other, characterized by typical low signal in T2- and T1-weighted images, diffusion restriction, increased enhancement in comparison to the normal-looking gland and extension of the changes beyond the glandular parenchyma [47, 48]. It is important to note that diffusion and enhancement changes may be subtle since normal glandular parenchyma also shows physiological enhancement and relative restriction of the diffusion. The infiltrative fibrosis and the lymphocytic infiltration are probably responsible for the signal characteristics.

Sjögren and IgG4-related diseases are clinically similar, but xerostomia is not so frequent and marked in the latter. Furthermore, Sjögren disease shows high apparent diffusion coefficient (ADC) values and mainly hyperintense T2 signal (i.e. absence of significant hypercellularity) due to multiple cystic components. Other differential diagnoses are with granulomatous diseases such as sarcoidosis that are very similar on images and should be distinguished using the clinical context and laboratory. Especially in the context of enlarged lymph nodes, a possible differential diagnosis includes lymphoma and sometimes biopsy is necessary to distinguish the two entities [48].

Other autoimmune parotitis cases, such as Kikuchi necrotising lymphadenitis and lupus lymphadenitis, can cause chronic involvement of the parotid glands together with reactive enlargement of the neck nodes (Fig. 7).

Noninflammatory masses of the salivary gland region in children

Lymphatic malformations

Lymphatic malformations (previously also known as lymphangioma or cystic hygroma) are vascular malformations that can be found in the head and neck regions and are typically transpatial (i.e. they involve several neck spaces); they can be microcystic, macrocystic or mixed and their pathogenesis is unknown [49]. Despite some confusion in literature, these are not tumors but are now considered malformations [50].

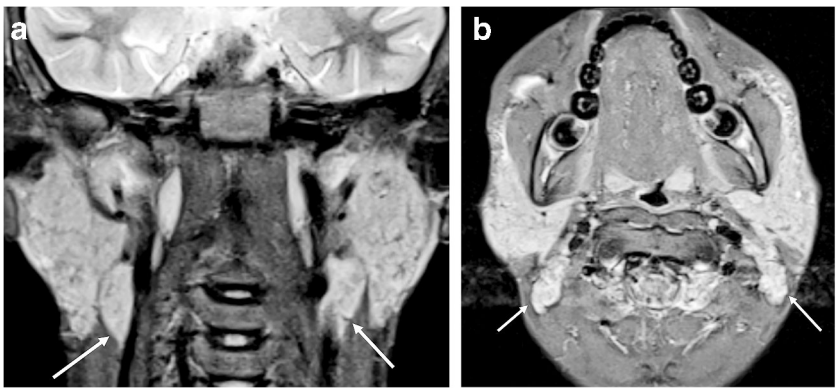

Fig. 7 An 8-year-old boy with Kikuchi necrotising lymphadenitis. **a, b** Coronal (**a**) and axial (**b**) STIR (short tau inversion recovery) images show bilateral and diffuse enlargement of the parotid glands with associated lymph-node involvement (*arrows*)

The lymphatic malformations involving the parotid spaces can be divided into Type I (involving the parotid space alone) and Type II (transpatial with involvement of the parotid space). Type II is far more frequent, but Type I can create some diagnostic problems [49]. Malformations can bleed spontaneously or after trauma and patients can have facial nerve symptoms [51–53].

Lymphatic malformations have three radiologic hallmarks (Fig. 8) [54, 55]:

1) multicystic structures (micro- or macrocysts) without contrast apart from thin cystic wall enhancement, with hyperintense content in T2-weighted images and variable signal in T1-weighted images depending on the proteinaceous content of the cysts.
2) fluid-fluid levels often present and due to internal bleeding.
3) transpatial extension.

However, problems in diagnosis, though rare, can arise when lymphatic malformation is characterized by a single cyst, is infected or develops a malignant transformation [56–58].

The main differential diagnosis is a 1st branchial cleft anomaly (a single cyst along the lateral profile of the parotid that can be associated with a tract) and haemangioma (an enhancing mass with internal flow voids).

Treatment is done using sclerotherapy or surgical removal [59].

Benign tumors

a) *Infantile hemangioma*

Different from lymphatic malformations, hemangiomas are considered neoplasms [26] and are the most common parotid tumors in children. In a study of 324 parotid masses in children, Bentz and colleagues [60] found that the most frequent neoplasms were hemangiomas (59%), followed by lymphatic malformations (27%) and other parotid tumors. Presentation is around 4 months of age. These neoplasms show rapid growth at the beginning and then an involutive phase before the second year of age. Infantile hemangiomas express GLUT1, which differentiates them from congenital hemangiomas that present at birth and can be non-involutive (NICH) or rapidly involutive (RICH) [61, 62]. Clinically, they may be superficial or deep, solitary or multiple, small or very large. They appear as red marks if superficial or more blue if deep. Deep lesions can also appear like a nodule with skin colour [63]. Radiologically, they show slightly hyperintense signal on T2-weighted images with multiple internal flow voids and homogenous enhancement that can become patchy in the involutive phase (Fig. 9). It is important to recognize the tubular shape of the flow voids to differentiate them from focal calcifications on MR (phleboliths), which are the radiologic hallmark of venous malformations (Fig. 10). No calcifications are visualized on CT that can instead show fatty content in the involutive phase [64, 65]. On US, hemangiomas appear as masses with packed vessels and high peaks on Doppler. MR angiography is not necessary unless PHACES (posterior fossa brain malformations, hemangioma, arterial lesions, cardiac abnormalities and eye abnormalities) syndrome is suspected [65]. Differential diagnosis includes other benign tumors, such as neurofibroma involving the facial nerve, but the age of presentation will be older, and, in pediatric population, these lesions are associated with neurofibromatosis Type 1 with typical areas of abnormal signal in brain (foci of abnormal signal intensity or FASI), sphenoid dysplasia, other plexiform neurofibromas and optic pathway gliomas within the brain [66].

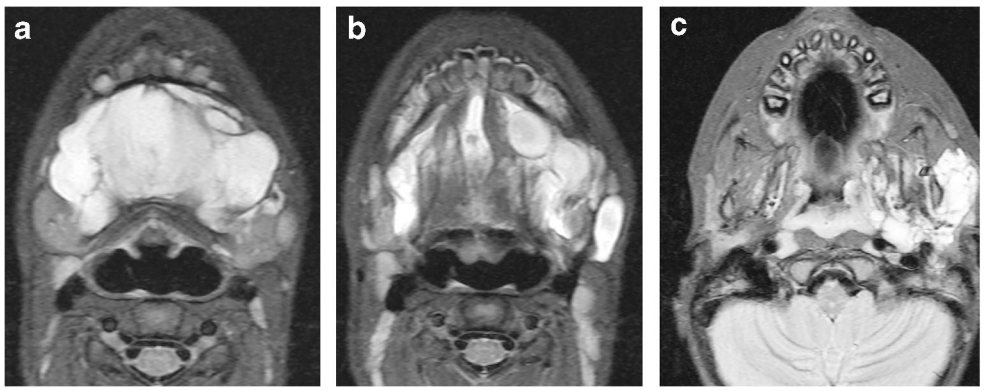

Fig. 8 A 33-month-old girl with macrocystic lymphatic malformation. **a–c** Axial STIR (short tau inversion recovery) images show involvement within the oral cavity (**a**), the left submandibular space (**b**) and left parotid space (**c**)

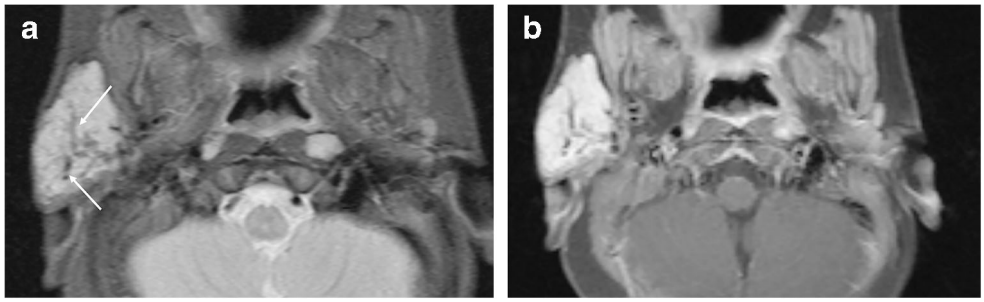

Fig. 9 Infantile haemangioma of the parotid gland in a 4-month-old girl. **a** Axial STIR (short tau inversion recovery) demonstrates enlargement of the parotid on the right with internal flow voids (*arrows*). **b** Axial T1-weighted image with fat saturation after injection of gadolinium shows homogeneous enhancement of the lesions and confirms the presence of multiple flow voids

b) *Pleomorphic adenoma*

Pleomorphic adenoma of the parotid gland, also known as benign mixed tumor of the parotid, is most common in adults between 30 and 60 years of age and has been described rarely in children [60]. This tumor can also involve other salivary glands [67]. Radiologic characteristics are the same as those described in adults and include a well-circumscribed intraparotid mass with hyperintense signal on T2-weighted images and a low T2 signal of the external capsule and homogenous enhancement [68] (Fig. 11). The signal on T2-weighted images can be extremely hyperintense, more than cerebrospinal fluid (CSF) and areas of internal necrosis with consequent heterogeneous enhancement of the neoplasm can develop in larger lesions (diameter >2 cm) [69]. Pleomorphic adenomas do not show diffusion restriction and can have internal calcifications visible on CT. Large pleomorphic adenomas typical extend medially with effacement of the parapharyngeal fat (Fig. 11).

Malignant tumors

a) *Rhabdomyosarcoma*

Rhabdomyosarcoma is the most common tumor of the soft tissues in children; however, parotid gland rhabdomyosarcomas are rare and often the involvement of the parotid space is secondary to an invasion from other sites [70]. It is still debated if the tumor originates from the gland or in the mesenchyme around it, but murine models have shown that salivary glands may contain a cell-of-origin of these aggressive neoplasms [71]. Nevertheless, in both pathology and imaging, some invasion of the periglandular soft tissue is expected and the most appropriate definition should be "rhabdomyosarcoma of the parotid region" [70]. These patients often do not have facial nerve symptoms and the presentation is as a painless mass; this is important to note clinically because delay in the diagnosis usually reduces the chances of total resection due to the local aggressiveness of the tumor [70, 72].

Imaging of rhabdomyosarcoma of the head and neck regions is characterized by bony invasion (better visible on CT), enhancement, nodal metastases, and intracranial and perineural invasion. Most of the rhabdomyosarcomas have internal areas of necrosis, which should always suggest a malignancy. Some reductions of the ADC values depending on the tumor cellularity have been described but they are not as low as other embryonal tumors of the head and neck region such as malignant rhabdoid tumors [73, 74] (Fig. 12).

b) *Mucoepidermoid carcinoma*

Mucoepidermoid carcinoma is the most frequent malignant tumor in the salivary glands in children. As with other malignant lesions involving the salivary glands, these neoplasms present as asymptomatic,

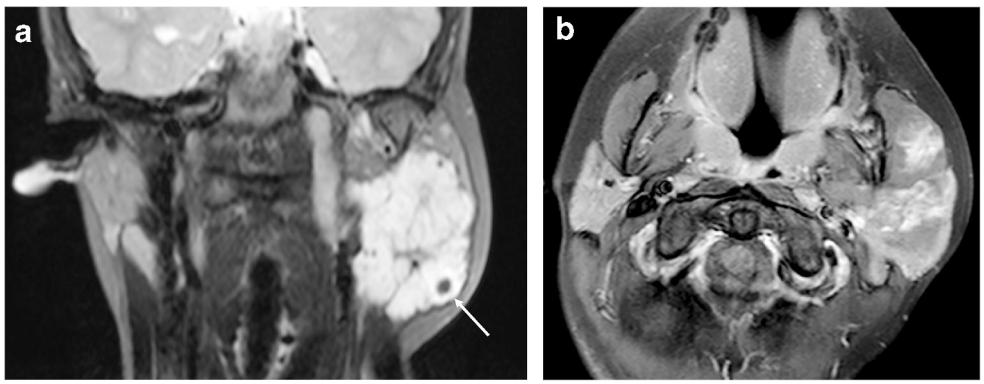

Fig. 10 A 6-year-old boy with large venous malformations of the left parotid space. **a** Coronal STIR (short tau inversion recovery) shows a phlebolith (*arrow*). **b** Axial T1-weighted with fat saturation post injection of gadolinium shows patchy, progressive enhancement typical of venous malformations. Note also the involvement of the masticator space

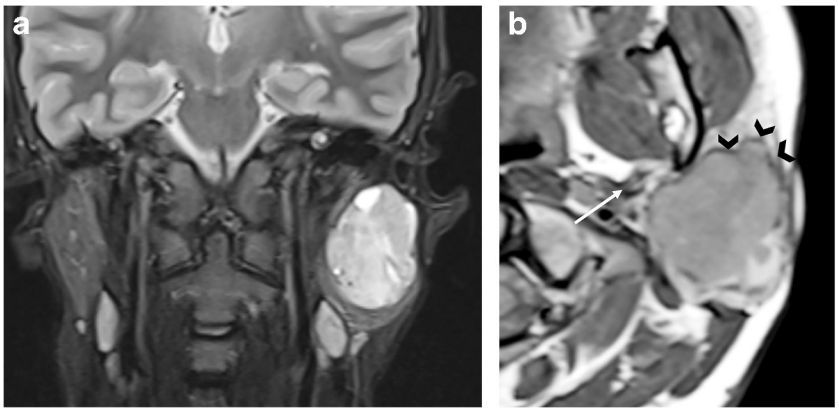

Fig. 11 A 14-year-old boy with left parotid pleomorphic adenoma. **a** Coronal STIR (short tau inversion recovery) image shows the mass appears well circumscribed with T2 heterogeneously hyperintense signal. **b** Axial T1-weighted image shows effacement of the left parapharyngeal fat (*arrow*) by the pleomorphic adenoma and demonstrates a hypointense external capsule (*arrowheads*)

slow-growing masses for several months before symptoms become apparent [75]. In the pediatric population, one of the possible risk factors is previous radiotherapy [76].

Imaging features are nonspecific and depend on the tumoral grade: Low-grade tumors are well-circumscribed masses within the parotid while higher-grade tumors present with local invasion and nodal metastases [77]. T2-weighted signal and post-contrast images also follow the tumor grade, which is more T2 hypointense in more cellular (i.e. aggressive) lesions and with clear areas of necrosis visible on both T2-weighted images and post-contrast sequences in more aggressive neoplasms (Figs. 13 and 14). Despite diffusion-weighted images being useful in predicting the cellularity, there is an overlap between benign and malignant tumors in the parotid region [78]. Low-grade mucoepidermoid carcinomas have an often pseudocystic appearance particularly on CT and US [27].

c) *Lymphoma*

Primary lymphomas of the salivary gland are uncommon in children and lymphomas account for only 1% of the parotid tumors. They are generally B-cell non-Hodgkin lymphomas and, in contrast to the adult counterpart, the prognosis in those cases is favourable [79]. They are considered mucosa-associated lymphoid tissues (MALT) lymphomas and are painless in most cases [27]. Radiologically, the most important characteristic is synchronous involvement of lymph nodes in the neck, which is often present. The disease can be unilateral or bilateral, diffuse or localized and the gland can present with heterogeneous hypointensity on T2-weighted images, variable T1 signal and diffusion restriction [27].

d) *Acinic cell carcinoma of the salivary glands*

Acinic cell carcinoma of the salivary gland accounts for about 15% of salivary gland malignancies; it is a low-grade malignant tumor characterised histologically by serous acinar cell differentiation of its neoplastic cells [80].

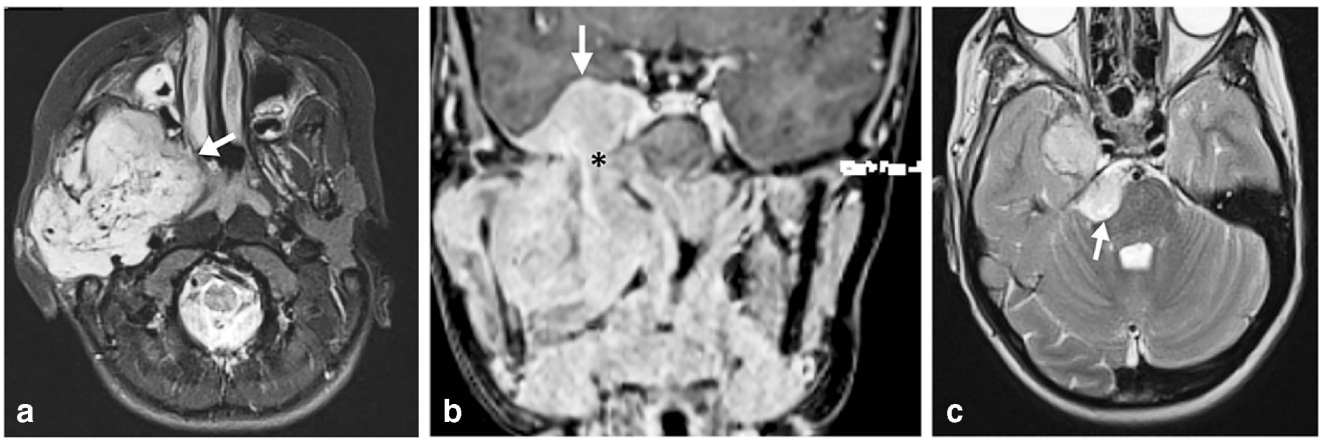

Fig. 12 A 9-year-old boy with rhabdomyosarcoma. **a** Axial STIR (short tau inversion recovery) image shows the large mass centred in the right parotid with extension medially in the masticator and carotid spaces and compression of the nasopharynx (*arrow*). Note multiple internal flow voids reflective of tumor high vascularity. The difference with haemangioma is in the aggressive nature of the lesion. **b** Coronal contrast-enhanced T1-weighted image with fat saturation shows enhancement of the lesion and demonstrates involvement of the skull base, the right foramen ovale (*), Meckel's cave and temporal dura (*arrow*). **c** Axial T2-weighted image shows the lesion (*arrow*) extending along the intracisternal trigeminal tract and compressing the pons on the right

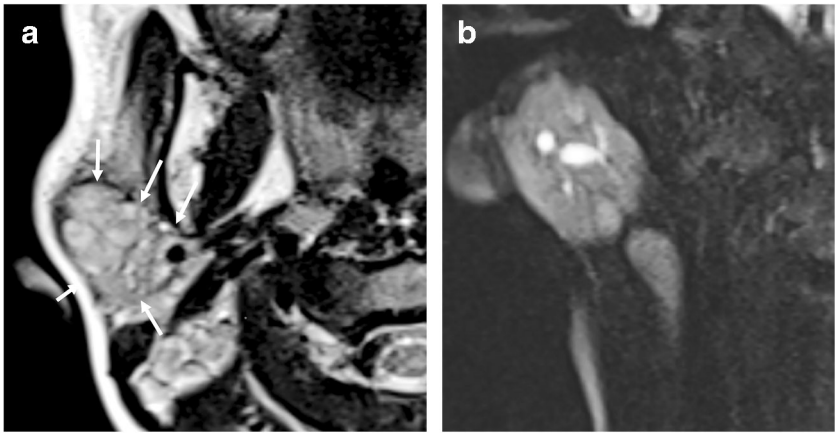

Fig. 13 Parotid secreting carcinoma in an 8-year-old girl. **a** Axial T2-weighted image shows a well demarcated mass (*arrows*) in the right parotid gland. **b** Coronal STIR (short tau inversion recovery) image demonstrates associated dilatation of the parotid ducts

It mainly involves the parotid gland (>80%), but can involve the other salivary glands as well as other head and neck spaces. Radiologically, these tumors are very similar to benign neoplasms involving the salivary gland and the diagnosis is histological [81] (Fig. 15).

Differential diagnosis of masses in the salivary spaces

Given the rarity of masses involving the salivary glands and/or surrounding tissues, differential diagnosis may be challenging when a mass in those areas is detected on radiologic examinations [82].

Here is an easy step-by-step approach to narrow down the diagnosis in case of neck masses involving salivary spaces as well as a diagnostic flowchart (Fig. 16). This is a general guide that must be used in view of the clinical context.

A few important considerations that the radiologist should take into account:

1) Is the mass solid or cystic?
2) If it is *solid,* as a general rule the signal characteristics, pattern of enhancement and internal structure are more useful in distinguishing the different entities.
3) If it is *cystic*, look at the location.

Fig. 14 Axial T1-weighted image after gadolinium injection and with fat saturation in a 12-year-old girl with aggressive mucopeidermoid carcinoma shows a large right parotid mass with marked enhancement and central necrosis

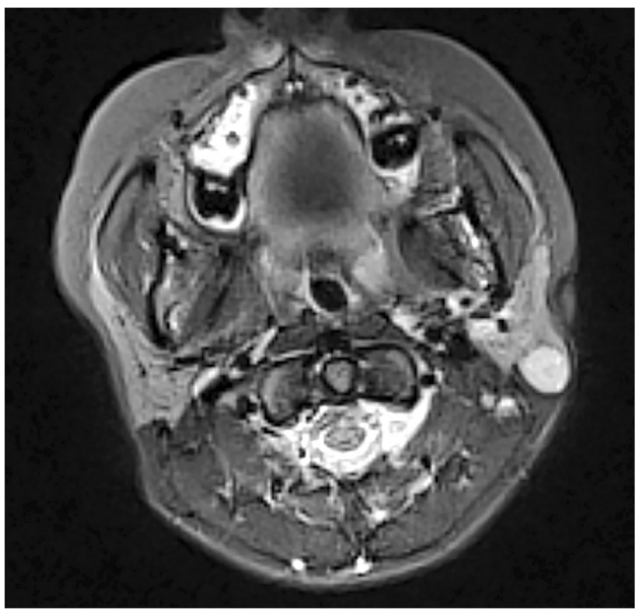

Fig. 15 Axial STIR (short tau inversion recovery) image shows an acinic cell carcinoma of the posterior aspect of the left parotid gland in a 12-year-old boy. The signal characteristics and sharp margins are similar to those of a pleomorphic adenoma

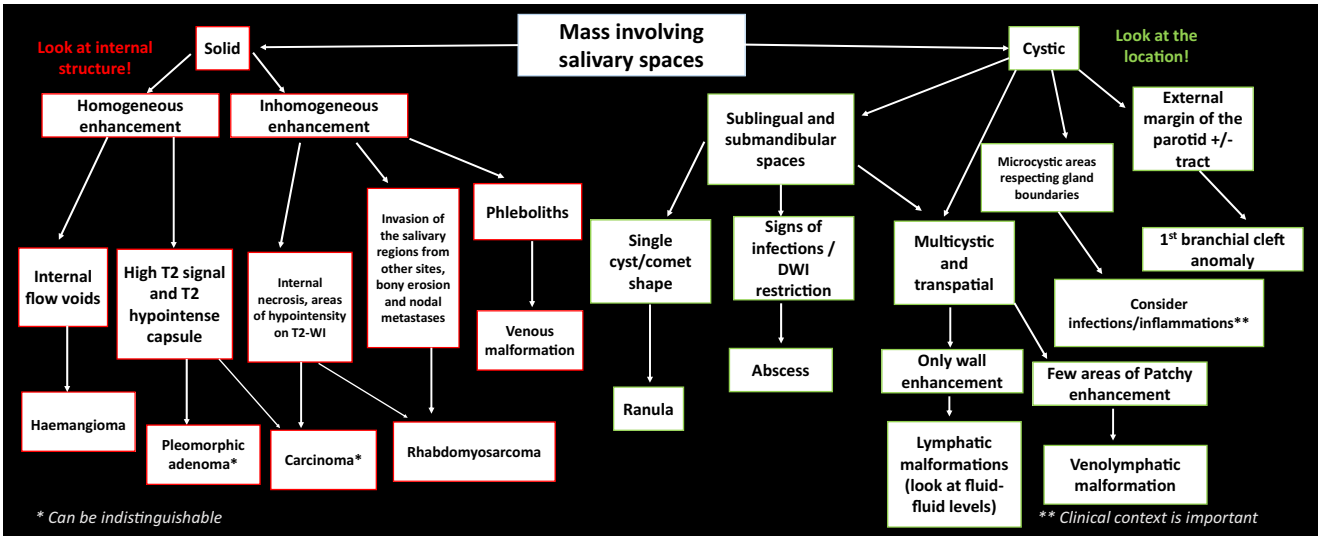

Fig. 16 A proposed flowchart helps differentiate salivary glands masses in children. *DWI* diffusion-weighted imaging, *T2-WI* T2-weighted imaging

Conclusion

Radiologic characterisation of lesions in the salivary glands of children is often challenging. Images are nonspecific and rarely indicated in inflammations/infections; however, some radiologic appearances may guide the differential diagnosis and avoid invasive procedures. A correct understanding of the signal and distribution characteristics of the masses involving the salivary spaces of the neck is very useful in distinguishing between benign and malignant entities.

Compliance with ethical standards

Conflicts of interest None

References

1. Weissman JL, Carrau RL (1998) Anterior facial vein and submandibular gland together: predicting the histology of submandibular masses with CT or MR imaging. Radiology 208:441–446
2. Boscolo-Rizzo P, Da Mosto MC (2009) Submandibular space infection: a potentially lethal infection. Int J Infect Dis 13:327–333
3. Otonari-Yamamoto M, Nakajima K, Tsuji Y et al (2010) Imaging of the mylohyoid muscle: separation of submandibular and sublingual spaces. AJR Am J Roentgenol 194:W431–W438
4. Ugga L, Ravanelli M, Pallottino AA et al (2017) Diagnostic work-up in obstructive and inflammatory salivary gland disorders. Acta Otorhinolaryngol Ital 37:83–93
5. Nanci A (2014) Ten Cate's oral histology - E-Book: development, structure, and function, 8th edn. Elsevier Health Sciences, Amsterdam
6. Miletich I, Som P (2015) Embryology of the salivary glands: An update. AJNR Am J Neuroradiol 5:167
7. Lehotay M, Kunkel M, Wehrbein H (2004) Lacrimo-auriculo-dento-digital syndrome. Case report, review of the literature, and clinical spectrum. J Orofac Orthop 65:425–432
8. Ferreira AP, Gomez RS, Castro WH et al (2000) Congenital absence of lacrimal puncta and salivary glands: report of a Brazilian family and review. Am J Med Genet 94:32–34
9. Chadi MJ, Saint Georges G, Albert F et al (2017) Major salivary gland aplasia and hypoplasia in Down syndrome: review of the literature and report of a case. Clin Case Rep 5:939–944
10. Yilmaz YF, Titiz A, Yurur-Kutlay N et al (2010) Congenital bilateral parotid gland agenesis in Klinefelter syndrome. J Craniomaxillofac Surg 38:248–250
11. D'Arco F, Youssef A, Ioannidou E et al (2020) Temporal bone and intracranial abnormalities in syndromic causes of hearing loss: an updated guide. Eur J Radiol 123:108803
12. Østerhus IN, Skogedal N, Akre H et al (2012) Salivary gland pathology as a new finding in Treacher Collins syndrome. Am J Med Genet A 158A:1320–1325
13. Teymoortash A, Hoch S (2016) Congenital unilateral agenesis of the parotid gland: A case report and review of the literature. Case Rep Dent 2016:2672496
14. D'Ascanio L, Cavuto C, Martinelli M, Salvinelli F (2006) Radiological evaluation of major salivary glands agenesis. A case report. Minerva Stomatol 55:223–228
15. Miyamoto RT, Hamaker RC, Lingeman RE (1976) Goldenhar syndrome. Associated with submandibular gland hyperplasia and hemihypoplasia of the mobile tongue. Arch Otolaryngol 102:313–314
16. Kumar KA, Mahadesh J, Setty S (2013) Dysgenetic polycystic disease of the parotid gland: Report of a case and review of the literature. J Oral Maxillofac Pathol 17:248–252
17. Finn DG, Buchalter IH, Sarti E et al (1987) First branchial cleft cysts: clinical update. Laryngoscope 97:136–140
18. Aronsohn RS, Batsakis JG, Rice DH, Work WP (1976) Anomalies of the first branchial cleft. Arch Otolaryngol 102:737–740
19. D'Souza AR, Uppal HS, De R, Zeitoun H (2002) Updating concepts of first branchial cleft defects: a literature review. Int J Pediatr Otorhinolaryngol 62:103–109
20. Bagchi A, Hira P, Mittal K et al (2018) Branchial cleft cysts: a pictorial review. Pol J Radiol 83:e204–e209
21. Adams A, Mankad K, Offiah C, Childs L (2016) Branchial cleft anomalies: a pictorial review of embryological development and spectrum of imaging findings. Insights Imaging 7:69–76
22. La'porte SJ, Juttla JK, Lingam RK (2011) Imaging the floor of the mouth and the sublingual space. Radiographics 31:1215–1230

23. Edwards RM, Chapman T, Horn DL et al (2013) Imaging of pediatric floor of mouth lesions. Pediatr Radiol 43:523–535
24. Ellis GL (2007) Lymphoid lesions of salivary glands: Malignant and Benign. Medicina Oral, Patología Oral y Cirugía Bucal. http://scielo.isciii.es/scielo.php?script=sci_arttext&pid=S1698-69462007000700003. Accessed 1 Apr 2020
25. Iro H, Zenk J (2014) Salivary gland diseases in children. GMS Curr Top Otorhinolaryngol Head Neck Surg 13:Doc06
26. Mehta D, Willging JP (2006) Pediatric salivary gland lesions. Semin Pediatr Surg 15:76–84
27. Inarejos Clemente EJ, Navallas M, Tolend M et al (2018) Imaging evaluation of pediatric parotid gland abnormalities. Radiographics 38:1552–1575
28. Jeffers L, Webster-Cyriaque JY (2011) Viruses and salivary gland disease (SGD): lessons from HIV SGD. Adv Dent Res 23:79–83
29. Yousem DM, Kraut MA, Chalian AA (2000) Major salivary gland imaging. Radiology 216:19–29
30. Chandak R, Degwekar S, Chandak M, Rawlani S (2012) Acute submandibular sialadenitis-a case report. Case Rep Dent 2012: 615375
31. Abdel Razek AAK, Mukherji S (2017) Imaging of sialadenitis. Neuroradiol J 30:205–215
32. Madani G, Beale T (2006) Inflammatory conditions of the salivary glands. Semin Ultrasound CT MR 27:440–451
33. Francis CL, Larsen CG (2014) Pediatric sialadenitis. Otolaryngol Clin N Am 47:763–778
34. Wei Y, Xiao J, Pui MH, Gong Q (2008) Tuberculosis of the parotid gland: computed tomographic findings. Acta Radiol 49:458–461
35. Razek AA, Castillo M (2010) Imaging appearance of granulomatous lesions of head and neck. Eur J Radiol 76:52–60
36. Garg R, Verma SK, Mehra S, Srivastawa AN (2010) Parotid tuberculosis. Lung India 27:253–255
37. Muccio CF, Caranci F, D'Arco F et al (2014) Magnetic resonance features of pyogenic brain abscesses and differential diagnosis using morphological and functional imaging studies: a pictorial essay. J Neuroradiol 41:153–167
38. Hammenfors DS, Valim V, Bica BERG et al (2020) Juvenile Sjögren's syndrome: clinical characteristics with focus on salivary gland ultrasonography. Arthritis Care Res (Hoboken) 72:78–87
39. Cimaz R, Casadei A, Rose C et al (2003) Primary Sjögren syndrome in the paediatric age: a multicentre survey. Eur J Pediatr 162:661–665
40. Ching AS, Ahuja AT (2002) High-resolution sonography of the submandibular space: anatomy and abnormalities. AJR Am J Roentgenol 179:703–708
41. Tonami H, Ogawa Y, Matoba M et al (1998) MR sialography in patients with Sjögren syndrome. AJNR Am J Neuroradiol 19: 1199–1203
42. Izumi M, Eguchi K, Uetani M et al (1998) MR features of the lacrimal gland in Sjögren's syndrome. AJR Am J Roentgenol 170:1661–1666
43. Means C, Aldape MA, King E (2017) Pediatric primary Sjögren syndrome presenting with bilateral ranulas: A case report and systematic review of the literature. Int J Pediatr Otorhinolaryngol 101: 11–19
44. Karim F, Loeffen J, Bramer W et al (2016) IgG4-related disease: a systematic review of this unrecognized disease in pediatrics. Pediatr Rheumatol Online J 14:18
45. Geyer JT, Ferry JA, Harris NL et al (2010) Chronic sclerosing sialadenitis (Küttner tumor) is an IgG4-associated disease. Am J Surg Pathol 34:202–210
46. Melo JC, Kitsko D, Reyes-Múgica M (2012) Pediatric chronic sclerosing sialadenitis: Küttner tumor. Pediatr Dev Pathol 15:165–169
47. Fujita A, Sakai O, Chapman MN, Sugimoto H (2012) IgG4-related disease of the head and neck: CT and MR imaging manifestations. Radiographics 32:1945–1958
48. De Cocker LJ, D'Arco F, De Beule T et al (2014) IgG4-related systemic disease affecting the parotid and submandibular glands: magnetic resonance imaging features of IgG4-related chronic sclerosing sialadenitis and concomitant lymphadenitis. Clin Imaging 38:195–198
49. Wiegand S, Zimmermann AP, Eivazi B et al (2011) Lymphatic malformations involving the parotid gland. Eur J Pediatr Surg 21: 242–245
50. Steiner JE, Drolet BA (2017) Classification of vascular anomalies: an update. Semin Interv Radiol 34:225–232
51. Som PM, Zimmerman RA, Biller HF (1984) Cystic hygroma and facial nerve paralysis: a rare association. J Comput Assist Tomogr 8:110–113
52. Lee GS, Perkins JA, Oliaei S, Manning SC (2008) Facial nerve anatomy, dissection and preservation in lymphatic malformation management. Int J Pediatr Otorhinolaryngol 72:759–766
53. Bhatt NK, Kang L-I, El-Mofty S et al (2018) Emergent parotidectomy after parotid lymphatic malformation hematoma. Otolaryngology Case Reports 7:16–18
54. Bansal AG, Oudsema R, Masseaux JA, Rosenberg HK (2018) US of pediatric superficial masses of the head and neck. Radiographics 38:1239–1263
55. Eren S, Bakir Z (2009) Imaging features of cervical lymphangiomas as a cause of respiratory distress and vascular-lymphatic disturbance. Eurasian J Med 41:39–43
56. Berry JA, Wolf JS, Gray WC (2002) Squamous cell carcinoma arising in a lymphangioma of the tongue. Otolaryngol Head Neck Surg 127:458–460
57. Linnaus ME, Notrica DM (2016) Infected cystic hygroma resulting in septic shock and respiratory failure: a case report. J Pediatr Surg Case Rep 9:19–22
58. Burusapat C, Sringkarawat S, Thanapurirat S et al (2018) An unusual presentation of idiopathic lymphatic cyst of the thigh. Case Rep Surg 2018:1–5
59. Tu JH, Do HM, Patel V et al (2017) Sclerotherapy for lymphatic malformations of the head and neck in the pediatric population. J Neurointerv Surg 9:1023–1026
60. Bentz BG, Hughes CA, Lüdemann JP, Maddalozzo J (2000) Masses of the salivary gland region in children. Arch Otolaryngol Head Neck Surg 126:1435–1439
61. Darrow DH, Greene AK, Mancini AJ et al (2015) Diagnosis and management of infantile hemangioma. Pediatrics 136:e1060–e1104
62. North PE, Waner M, Mizeracki A, Mihm MC Jr (2000) GLUT1: a newly discovered immunohistochemical marker for juvenile hemangiomas. Hum Pathol 31:11–22
63. Smith CJF, Friedlander SF, Guma M et al (2017) Infantile hemangiomas: an updated review on risk factors, pathogenesis, and treatment. Birth Defects Res 109:809–815
64. Vilanova JC, Barceló J, Smirniotopoulos JG et al (2004) Hemangioma from head to toe: MR imaging with pathologic correlation. Radiographics 24:367–385
65. Bhat V, Salins PC, Bhat V (2014) Imaging spectrum of hemangioma and vascular malformations of the head and neck in children and adolescents. J Clin Imaging Sci 4:31
66. Rai A, Kumar A (2015) Neurofibroma of facial nerve presenting as parotid mass. J Maxillofac Oral Surg 14:465–468
67. Ahmedi JR, Ahmedi E, Perjuci F et al (2017) Pleomorphic adenoma of minor salivary glands in child. Med Arch 71:360–363
68. Ikeda K, Katoh T, Ha-Kawa SK et al (1996) The usefulness of MR in establishing the diagnosis of parotid pleomorphic adenoma. AJNR Am J Neuroradiol 17:555–559
69. Rodriguez KH, Vargas S, Robson C et al (2007) Pleomorphic adenoma of the parotid gland in children. Int J Pediatr Otorhinolaryngol 71:1717–1723

70. Walterhouse DO, Pappo AS, Baker KS et al (2001) Rhabdomyosarcoma of the parotid region occurring in childhood and adolescence. A report from the Intergroup Rhabdomyosarcoma Study Group. Cancer 92:3135–3146
71. Geltzeiler M, Li G, Abraham J, Keller C (2015) The case for primary salivary rhabdomyosarcoma. Front Oncol 5:74
72. Renick B, Clark RM, Feldman L (1988) Embryonal rhabdomyosarcoma: presentation as a parotid gland mass. Oral Surg Oral Med Oral Pathol 65:575–579
73. Kralik SF, Haider KM, Lobo RR et al (2018) Orbital infantile hemangioma and rhabdomyosarcoma in children: differentiation using diffusion-weighted magnetic resonance imaging. J AAPOS 22:27–31
74. Freling NJM, Merks JH, Saeed P et al (2010) Imaging findings in craniofacial childhood rhabdomyosarcoma. Pediatr Radiol 40: 1723–1738
75. Sultan I, Rodriguez-Galindo C, Al-Sharabati S et al (2011) Salivary gland carcinomas in children and adolescents: a population-based study, with comparison to adult cases. Head Neck 33:1476–1481
76. Loy TS, McLaughlin R, Odom LF, Dehner LP (1989) Mucoepidermoid carcinoma of the parotid as a second malignant neoplasm in children. Cancer 64:2174–2177
77. Kashiwagi N, Dote K, Kawano K et al (2012) MRI findings of mucoepidermoid carcinoma of the parotid gland: correlation with pathological features. Br J Radiol 85:709–713
78. Christe A, Waldherr C, Hallett R et al (2011) MR imaging of parotid tumors: typical lesion characteristics in MR imaging improve discrimination between benign and malignant disease. AJNR Am J Neuroradiol 32:1202–1207
79. Choi J, Choi HJ, Yim K et al (2018) Pediatric follicular lymphoma of the parotid gland. Arch Craniofac Surg 19:279–282
80. Al-Zaher N, Obeid A, Al-Salam S, Al-Kayyali BS (2009) Acinic cell carcinoma of the salivary glands: a literature review. Hematol Oncol Stem Cell Ther 2:259–264
81. Sepúlveda I, Frelinghuysen M, Platin E et al (2015) Acinic cell carcinoma of the parotid gland: a case report and review of the literature. Case Rep Oncol 8:1–8
82. Gaunt T, D'Arco F, Smets AM et al (2019) Emergency imaging in paediatric oncology: a pictorial review. Insights Imaging 10:120